ELSEVIER

Applied Surface Science 181 (2001) 211–224

applied surface science

www.elsevier.com/locate/apsusc

Characterization of uranium oxide thin films grown from solution onto Fe surfaces

S.R. Qiu[a,b], C. Amrhein[b], M.L. Hunt[b], R. Pfeffer[c], B. Yakshinskiy[c], L. Zhang[c], T.E. Madey[c], J.A. Yarmoff[a,*]

[a]*Department of Physics, University of California, Riverside, CA 92521, USA*
[b]*Department of Environmental Sciences, University of California, Riverside, CA 92521, USA*
[c]*Department of Physics and Astronomy, and Laboratory for Surface Modification, Rutgers, The State University of New Jersey, Piscataway, NJ 08854, USA*

Received 23 March 2001; accepted 15 June 2001

Abstract

A novel method has been discovered for growing uranium oxide films onto iron substrates from solution. The films were characterized by X-ray photoelectron spectroscopy, X-ray diffraction, scanning electron microscopy, Rutherford backscattering spectrometry, and near-edge X-ray absorption fine structure. The as-grown films appear to be iridescent. They are composed of an amorphous uranium(VI) oxide with water incorporated, and are most likely a partially dehydrated schoepite. Topographic images reveal that the surfaces of the films are basically flat, but contain some small hills and valleys. Small cracks are distributed randomly across the surfaces. Upon heating in vacuum, the films crystallize and reduce to a uranium(IV) oxide, and the cracks enlarge. When a heated sample is exposed to air, the surface re-oxidizes to uranium(VI) while the bulk remains as crystalline uranium(IV) oxide.

Keywords: Uranium oxide; X-ray diffraction; Rutherford backscattering spectrometry; Scanning electron microscopy; X-ray photoelectron spectroscopy; Zero-valent iron

1. Introduction

The manufacture of nuclear weapons and fuel-grade uranium has produced tremendous amounts of radioactive waste materials that are being stored at DOE complexes and reactor sites throughout the United States. Spent nuclear fuel is typically 95–99% UO_2, while the remaining fraction is composed of fission products and transuranic elements that formed during reactor operation [1]. Studies on the corrosion rates and reaction products of spent nuclear fuel have found several uranyl phases depending upon the temperature, humidity, and oxygen pressure. Surface coatings that have been identified on corroding fuel pellets include U_4O_9, U_3O_7, dehydrated schoepite $[(UO_2)O_{0.25-x}(OH)_{1.5+2x}$ (where $0 \leq x \leq 0.25$)], and U_3O_8 [2–4]. Leakage from underground storage of radioactive wastes has led to the introduction of radioactive contaminants, including uranium, into the groundwater in the vicinity of many of the DOE sites. Contaminated sites include Hanford, WA, Snake River Aquifer, ID and Bear Creek in Oak Ridge, TN. In order to remove the contaminants from soils, sediments, and groundwaters, it is essential

* Corresponding author. Tel.: +1-909-787-5336; fax: +1-909-787-4529.
E-mail address: yarmoff@ucr.edu (J.A. Yarmoff).

0169-4332/01/$ – see front matter
PII: S0169-4332(01)00385-3

to have a complete understanding of the interactions of the contaminants and their compounds with the environment and with the materials that are used for remediation.

Zero-valent iron (ZVI) is a leading candidate material for the use in cleaning up groundwater contaminants [5]. Most aqueous contaminants are in their fully oxidized forms when in the environment. It has been widely believed that ZVI removes contaminants by a surface chemical reduction reaction, which immobilizes them. In earlier studies, however, it was found that although many aqueous contaminants (including U) are deposited onto Fe surfaces by reduction [6–8], uranyl ions may also be removed by non-reductive precipitation [6]. In [6], untreated Fe foil was reacted in an aqueous solution containing uranyl ions. Following reaction, the foil was probed with X-ray photoelectron spectroscopy (XPS), which showed that uranium was deposited onto the surface as U(VI), i.e., without reduction. It was also found that the amount of uranium deposited on the surface is very sensitive to the dissolved gases in solution. If atmospheric gases were present in the solution, a 10 Å thick uranium oxide film was deposited onto the surface. When the dissolved atmospheric gases were removed from solution, however, a much thicker film, composed of a U(VI) oxide, formed on the surface. The film was thick enough that no XPS Fe signal was detectable from the substrate. Presumably, the important gas being purged during growth is CO_2, which readily reacts with uranium in solution to form uranyl-carbonate complexes.

This technique for growing thick uranium oxide films from solution provides a method of sample preparation that will enable other kinds of experiments involving uranium oxide surfaces [6]. The films are thin enough that the radioactivity is negligible compared to that associated with bulk uranium oxides, thereby making it less hazardous for use in a variety of laboratories. This opens up new opportunities for research involving uranium oxide surfaces, such as investigating the chemical reactivity of the materials and the effects of radiation on the surface composition and chemistry. In addition, these materials can be exposed to environmental conditions, such as those found in underground storage and in the vadose zone, in order to ascertain the stability of uranium oxides.

To effectively utilize the uranium oxide films, however, they must be carefully characterized with respect to their physical and chemical properties. In this work, films grown from solution onto Fe substrates were investigated by a variety of techniques. The techniques include XPS, X-ray diffraction (XRD), Rutherford backscattering spectrometry (RBS), scanning electron microscopy (SEM), low energy ion scattering (LEIS), and near-edge X-ray absorption fine structure (NEXAFS). The combination of these techniques enables the determination of the physical and chemical properties of both the bulk and surface regions of the film.

The results of the different techniques are in general agreement with each other, and suggest that the as-grown film is an amorphous uranium(VI) oxide with a certain amount of incorporated water, tentatively identified as a partially dehydrated schoepite. The thickness of the films is in the order of 1 μm, and there are small cracks distributed across the film surface. When heated in vacuum, the film reduces to a uranium(IV) oxide and crystallizes, while the cracks enlarge. Heating does not affect the general morphology of the film surface, however. Upon exposure to air, the surface re-oxidizes to uranium(VI), but the bulk of the material remains a crystalline uranium(IV) oxide.

2. Experimental procedures

The uranium oxide films were grown in solution by reacting iron foil (Alfa Aesar, 99.99%) in 200 ml of a 1 mM uranyl nitrate solution at pH 5 for 3 h. The iron foil was stored in a vacuum desiccator prior to reaction. No modification was made to the foil surface before reaction, i.e., the native oxide was intact. Acetone and methanol were used to remove grease from the foil surface before inserting the foil into the solution. Deionized water was deaerated with high purity (99.99%) Ar gas for more than 24 h before mixing with the uranyl nitrate powder. The uranyl nitrate solution was continuously purged with the Ar during the entire reaction to prevent O_2 and CO_2 dissolution. The solution pH was adjusted to 5 before reaction, but was not further controlled. The pH at the end of reaction increased only slightly to 5.3. After the 3 h reaction, the sample was pulled out and dried in air. Although different samples were used for RBS and LEIS than for XPS, NEXAFS, XRD, and SEM, the growth conditions were the same for all of the samples.

The morphology of the surfaces was investigated with SEM. The instrument (Philips Model XL30-FEG), which is equipped with both secondary electron (SE) and backscattered electron (BSE) detectors, was operated at 30 kV. Images were acquired in both the SE and BSE modes with the sample normal to the electron beam. The concentrations of each element present in the film were estimated by energy dispersive X-ray (EDX) analysis. SEM was also used to estimate the thickness of the as-grown film. To do this, the sample was mounted 45° off normal and rotated in such a way that the edge of the film could be seen. The thickness of the film was then determined by estimating the height of the film edge from the image.

XPS was performed in a stainless steel ultra-high vacuum (UHV) chamber with a base pressure of 1×10^{-10} Torr. The details of this system are described elsewhere [6]. The sample was mounted onto a sample holder equipped with e-beam heating and a K-type thermocouple. To insure that the surface oxidation states were not altered during the sample transfer from solution to the UHV chamber, a reaction vessel was setup inside a glove bag filled with Ar for some of the measurements. The glove bag was attached directly to a load lock door on the transfer chamber. In this manner, the sample was kept entirely under an inert atmosphere while being moved from the solution into the UHV chamber.

NEXAFS spectra were collected on beamline 4-1 of the Stanford Synchrotron Radiation Laboratory (SSRL). The sample was kept at room temperature during the measurements. A Si(2 2 0) double crystal monochromator with a 1 mm upstream aperture was used as an excitation source, while fluorescence was employed to monitor absorption. Fluorescence data were collected for all samples using a Canberra 13-element Ge detector. The samples and standards were analyzed at an angle of approximately 45° to the incident beam. Inert gases (N_2 or Ar) were used to fill the ionization chamber before and after the samples and standards were introduced. Commercial UO_3 (CERAC, 99.8% purity) and UO_2 (Johnson Matthey, 99.8% purity) bulk materials were used as the standards.

A 2.06 MeV He^{++} ion beam was used for the RBS measurements. The sample was mounted at the center of the stage of a 2-axis goniometer that is located in the channeling beamline of a General Ionex Model 4117 Tandetron accelerator. The He^{++} ion beam was normal to the sample surface, and the backscattered ions were recorded with a Si surface barrier detector mounted at an angle of 165° from the incident beam direction. The beam was collimated to a rectangular spot approximately 1 mm × 2 mm. The combined energy resolution of the beam, detector and electronics was about 20 keV. RBS data were recorded over 512 channels at a rate low enough to keep pulse pileup negligible.

XRD spectra were collected in continuous step scan mode using a Siemens D500 diffractometer with Cu Kα radiation. A Digital PDP11 microcomputer was interfaced to the diffractometer via a DACO–MP interface. DIFFRAC-AT software was used to collect, process, and analyze the XRD spectra. The X-ray scans for all samples were run at 3.5 s per 0.01° as 2Θ was scanned from 2.00° to 90.00°. All samples were run in air. The spectra were background subtracted and numerically smoothed.

To monitor the changes of the uranium oxide surface species with annealing temperature, LEIS measurements were performed in a separate UHV chamber, which had a base pressure of 1×10^{-10} Torr [9]. A differentially pumped sputter ion gun was used as the He^{+} ion source and a 100 mm radius concentric hemispherical analyzer (CHA) was employed to detect the scattered ions. The incident ion flux was 1×10^{14} ions/cm^2. The scattering angle was 135° and the CHA analyzer was operated in the fixed retardation mode with a retarding ratio of 5.

3. Results

Before reaction, the Fe foils had the usual shiny, metallic color, but after 3 h of reaction in the uranyl solution and drying in air, they appeared iridescent. Fig. 1(a) shows a photograph of a foil before reaction, while photographs of two reacted foils are shown in Fig. 1(b); one is navy blue and the other is orange-red. This suggests that the film thickness is in the order of the wavelength of visible light, and that the color is due to the interference of the light reflecting from the top and bottom surfaces of the film.

The microscopic surface morphology is revealed by the SEM images, which are shown in Fig. 2. SE images are shown at different lateral resolutions in

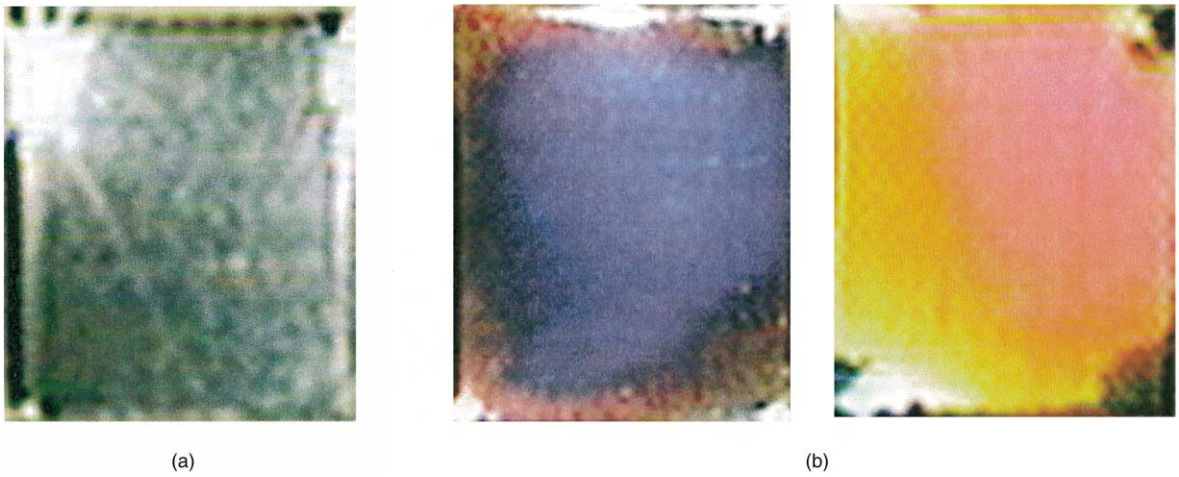

Fig. 1. Photographs of: (a) an Fe foil before reaction; (b) two samples following uranium oxide film growth.

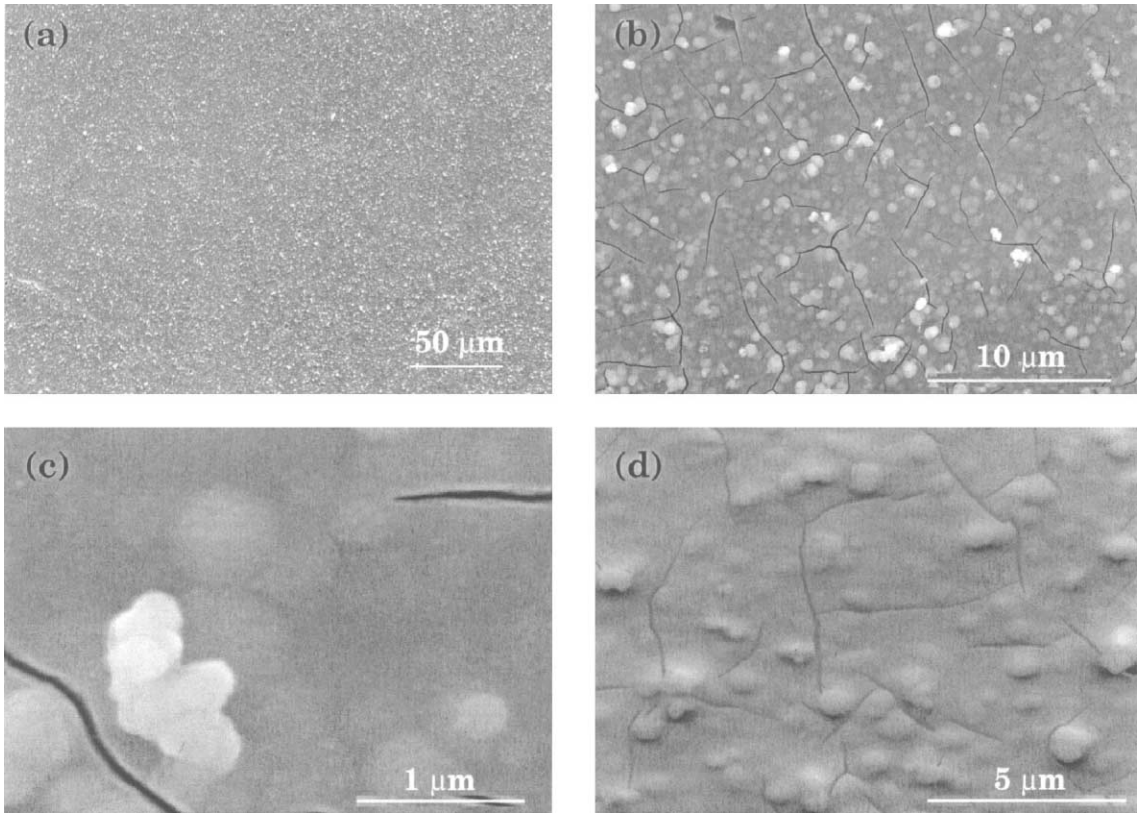

Fig. 2. Representative SEM images collected from the as-grown uranium oxide film. (a)–(c) are SE images with increasing in resolution, (d) is the BSE image. The beam energy was 30 keV.

Fig. 2(a)–(c). The surface of the film is generally flat, but it contains many circular protrusions, in the order of 1 μm in diameter, which are visible as bright spots across the surface of the film. There are also a number of cracks in the films. The width of the cracks is in the order of nanometers, with the largest one being 70 nm wide.

Since the SE signal depends on both the chemical composition and topography of the imaged area, however, it cannot be used reliably to characterize the chemical homogeneity of a sample. To reveal the compositional homogeneity of the films, BSEs were employed. Images were collected with a dedicated solid-state BSE detector operated in Z-contrast mode with a spatial resolution in the order of 0.1 μm [10]. The protrusions seen in the images are in the order of 1 μm in diameter, which implies that BSE imaging can successfully characterize the chemical homogeneity of the film. A BSE image in Z-contrast mode was collected from the as-grown film and is displayed in Fig. 2(d). The similar intensity of the protrusions and the surrounding flat areas is strong evidence that the small protrusions have the same chemical composition and density as the rest of the film. This was confirmed also by EDX spot analyses, which did not show any difference in the composition of the protrusions and the flat areas. The fact that some protrusions appear much brighter in SE mode is due to the fact that edges and small grains always appear brighter in SE due to the decreased absorption and consequently stronger signal caused by a reduced interaction volume as compared to flat areas.

In order to estimate the thickness of the films, a region was intentionally peeled away by cutting the sample. The sample was then placed at 45° angle from normal so that the edge of the film could be viewed. Edge-view images are shown at different resolutions in Fig. 3(a)–(c). The film appears dark, while the substrate is bright. The edge of a film is clearly seen in these images, from which the height is estimated to be in the range of 450–700 nm.

SE images collected from a sample that was annealed in vacuum at 450°C for 10 min are shown in Fig. 4(a)–(c). The general morphology is similar to that of the as-grown material, but the cracks have increased in number and became enlarged, with some approaching a width of 1 μm.

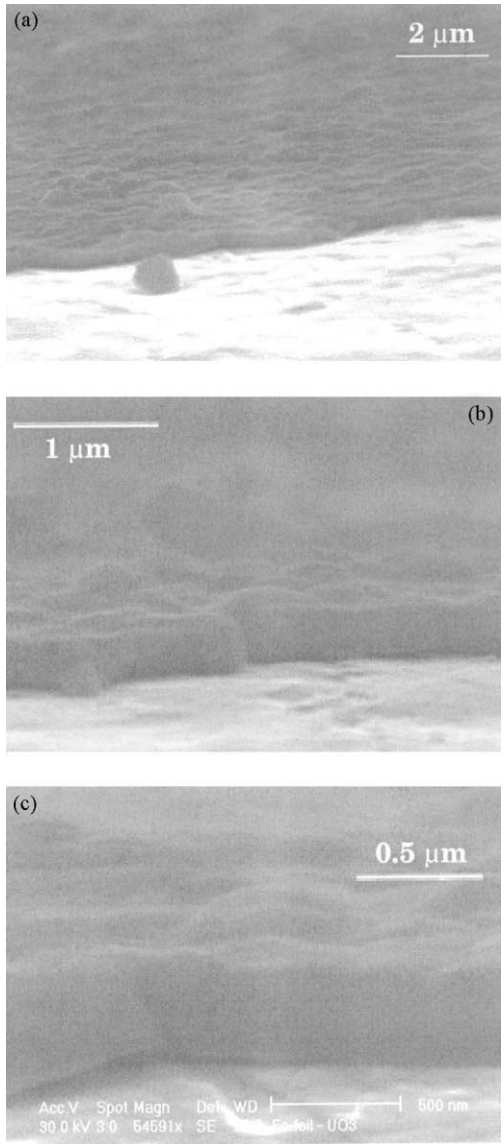

Fig. 3. Side view SEM images collected from the as-grown uranium oxide film. The beam energy was 30 keV. The resolution of the images increases from the top to the bottom. The thickness of the film can be estimated from this view.

EDX showed uranium, oxygen and iron as the major elements comprising both the as-grown and heated samples. The Fe signal is attributed to the substrate Fe foil. The escape depth of the X-rays is larger than the film thickness, so the Fe EDX signal could come from Fe visible through the film, or from

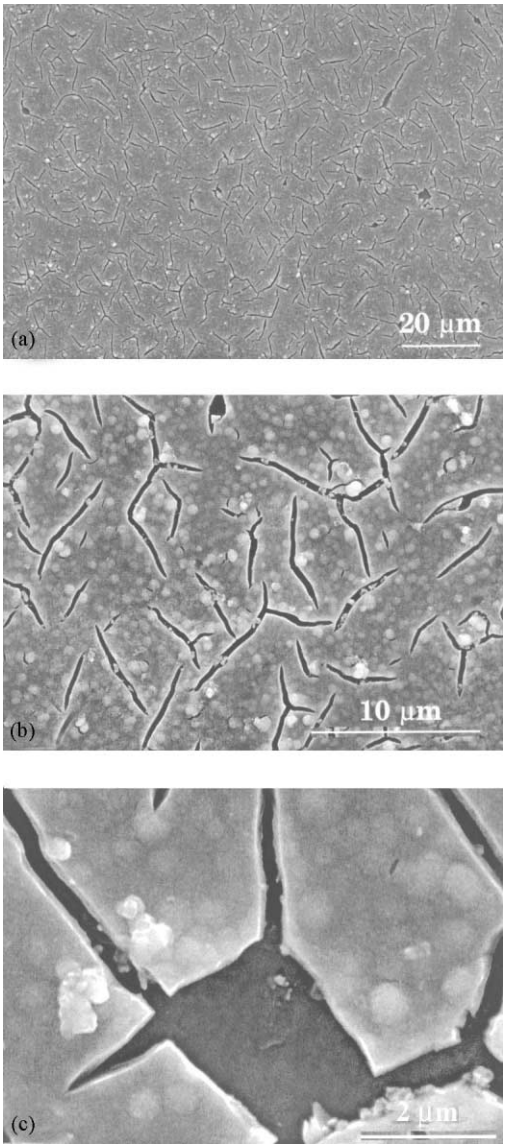

Fig. 4. Representative SEM images collected from a uranium oxide film that was heated in vacuum to 450°C for 10 min. All images are collected from SEs. The beam energy was 30 keV. The resolution of the images increases from the top to the bottom.

substrate Fe exposed by the cracks. The U to O ratio of the film is difficult to determine from the EDX data, since native Fe oxides exist on the substrate before reaction and the substrate itself may have been further oxidized during reaction. However, the results do show that the as-grown film consists solely of uranium and oxygen. Note, however, that H cannot be excluded based upon the EDX results. In addition, some C was found in the annealed sample. This suggests that uranium carbonate, which is a stable uranium compound, may have formed on the surface by reaction with atmospheric CO_2 when the sample was exposed to air after heating in vacuum and prior to insertion into the SEM instrument.

The chemical composition of the surface region of the film was determined from XPS. The unreacted samples were covered with a layer of Fe(III) oxide, i.e., Fe_2O_3, which was thick enough to obscure the Fe metal below [6]. After reaction, however, the surface was completely covered with a uranium oxide film. A survey scan collected from the as-grown film is shown in Fig. 5. The only photoelectron signals observed can be assigned to uranium, oxygen and carbon core levels. Neither Fe photoemission nor Fe Auger signals are present in the spectra. The lack of any measurable Fe signal confirms that a relatively thick uranium oxide film has formed on the Fe substrate. The relative intensities of the XPS peaks indicate that the surface of the film is composed primarily of uranium and oxygen, with a trace amount of carbon.

A blow-up of the U 4f region of the as-grown sample is shown in spectrum (a) of Fig. 6. The U $4f_{7/2}$ peak of the as-grown material has a binding energy of 381.8 eV, which is indicative of the U(VI) oxidation state, as discussed previously [6]. An XPS spectrum collected after annealing the sample in vacuum at 450°C for 10 min is shown in trace (b) of Fig. 6. After annealing, the U 4f peaks shift towards lower binding energy by almost 2 eV, and a satellite, which is marked with an arrow, appears at an apparent binding energy of 386.5 eV. The binding energy shift and the satellite feature are in excellent agreement with XPS spectra collected previously from a single crystal of UO_2 [9]. Thus, it can be concluded that heating the sample in vacuum removes oxygen from the film, thereby reducing it to a U(IV) oxide. Spectrum (c) in Fig. 6 was collected from the annealed surface following exposure to air for 5 days. After the air exposure, the U 4f peak shifted back towards higher binding energy and the satellite feature disappeared. The binding energy of the peak in spectrum (c) of Fig. 6 is identical to that of spectrum (a), which suggests that air exposure re-oxidizes the surface region to U(VI).

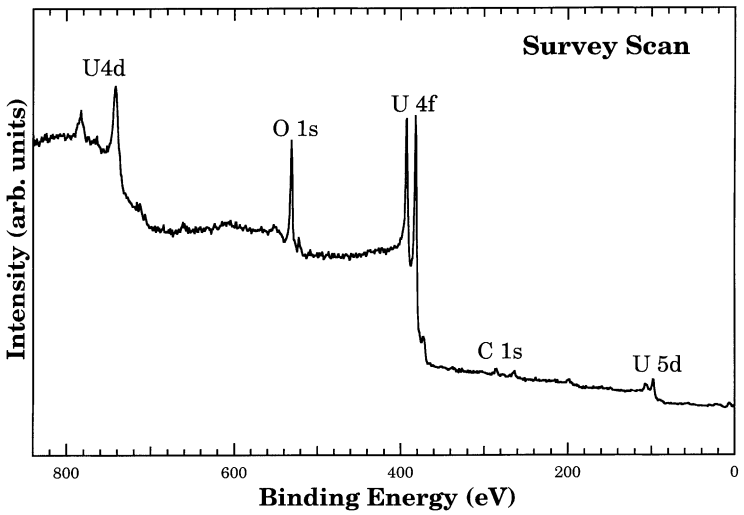

Fig. 5. XPS survey spectra collected from the surface of an as-grown uranium oxide film.

Additional support for the notion that the uranium is deposited from solution as U(VI), rather than as U(IV), was provided by the following experiment. Although it is clear from XPS that the surface region of the film is composed of U(VI), there is a possibility that uranium was first deposited from solution onto the surface in the reduced form, i.e., U(IV), but then the surface species re-oxidized to (VI) during the sample transfer from air to UHV. To determine whether the air exposure modified the surface species, a set of measurements was performed on samples that were reacted inside of a glove bag. The glove bag was purged with a constant flow of high purity Ar gas so that the reacted sample had no exposure to air during the entire transfer from solution to the UHV chamber. The XPS spectra collected after reaction in the glove bag showed the same uranium oxidation state as was obtained following transfer through air. Thus, reaction with air during the transfer can be ruled out as contributing to U(VI) formation. In addition, the surface reacted in the glove bag was found to be nearly carbon-free, which suggests that the trace amount of carbon observed on other samples was picked up during the transfer through air.

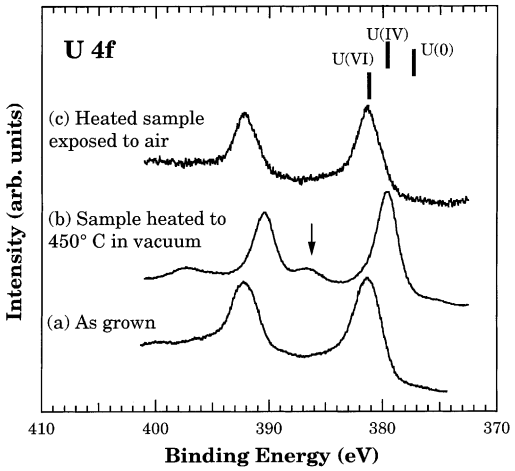

Fig. 6. U 4f XPS spectra obtained from uranium oxide films at various stages, as indicated in the legend.

NEXAFS is a much more bulk-sensitive technique than XPS, and the results indicate that the oxidation states observed in XPS are consistent throughout the bulk of the film. NEXAFS spectra collected from samples and standards are shown in Fig. 7, in which they are plotted on a relative energy scale with the U(IV) L_{III} edge assigned as 0. The absorption edge was defined at the half-height, which was determined by the derivative of the spectrum after normalization to the maximum above-edge intensity. The spectrum collected from the as-grown sample has the same features as that from the standard UO_3 powder, as shown in spectra (a) and (b) of Fig. 7. The edge position (vertical line A) is the same in both spectra, and is shifted about 4 eV towards higher energy than

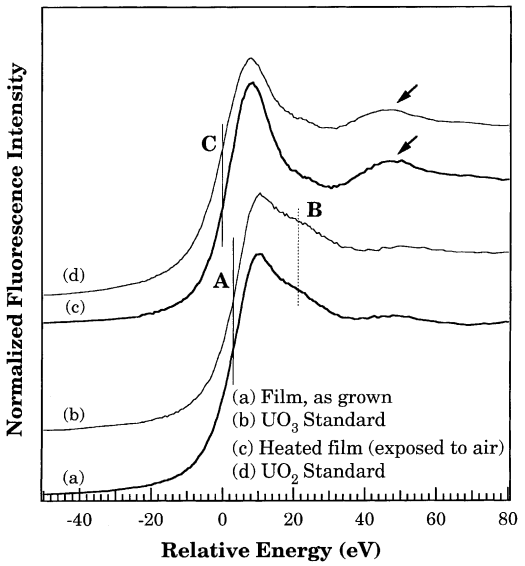

Fig. 7. NEXAFS spectra at the U L_{III} edge collected from various uranium oxide films. Specifications are shown in the legend. The horizontal axis is a relative energy scale with the U(IV) edge defined as 0.

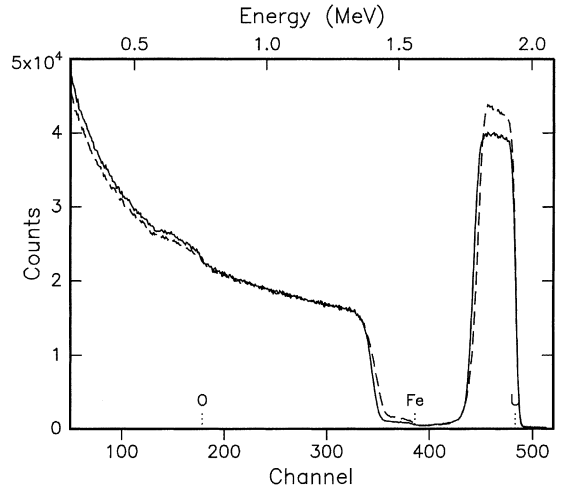

Fig. 8. Comparison of pre- and post-anneal RBS spectra collected from uranium oxide films, normalized to the same Fe substrate signal.

the U(IV) edge (vertical line C). Also, a shoulder at about 20 eV above the U(IV) edge is discernable in both spectra, as indicated by line B. These features confirm that the uranium in the as-grown film is indeed in the U(VI) oxidation state [11,12]. This does not rule out the possibility, however, that a very thin layer of U(IV) exists adjacent to the iron substrate. Furthermore, the spectrum collected from the heat-treated sample is identical to the standard U(IV) material (spectra (c) and (d) in Fig. 7). Both have the same edge position and post-edge features, as indicated by line C and the arrows. Note that there may be a small feature at a binding energy close to feature B in spectra (c) and (d), but it is not as pronounced as it is in spectra (a) and (b). Thus, it is concluded that the bulk of the film is converted to U(IV) upon heating in vacuum.

RBS was used as a quantitative measure of the bulk composition and thickness of the uranium oxide films. The analysis was performed by matching the RBS data to the simulated spectra generated with the RUMP RBS analysis software package [13,14]. The RBS spectra collected from the as-grown film (solid line) and after a light anneal at 235°C for 1 h in 1 atm of flowing N_2 (dashed line) are shown in Fig. 8. U, Fe, and O edges can be seen in the spectra. The U and O edges are at the elastic energies, which are marked with dashed vertical lines, which indicate that U and O are present at the outermost surface. Because the Fe substrate is buried beneath the film, the Fe edge has its main intensity well below the elastic energy. There is, however, a small edge at the Fe elastic energy, which indicates that there is either some Fe incorporated in the U oxide film, or that the surface of the Fe substrate is directly visible through holes or cracks in the film.

The stoichiometry of the film was determined by integration of the respective peaks. In order to integrate the O peak, a background was subtracted, which was modeled by a 4th-order polynomial fit to the surrounding substrate signal. The spectrum collected from the as-grown sample showed a layer whose O:U ratio was about 4.5. The intensities of the U and O peaks could only be normalized to the Fe substrate signal, however, by postulating the presence of an undetectable light constituent in the film, which can be assumed to be hydrogen. With this assumption, the film would have a composition of $[UO_3]_1 + [H_2O]_{1.5} + Fe_{0.15}$. Note that the Fe signal is most likely not due to incorporation of Fe within the film, but is more likely due to the presence of pinholes or cracks exposing some of the substrate, consistent with the cracks seen in SEM images. The UO_3 constituent is calculated to have an areal density (total U + O atoms) of about 1×10^{18} atoms/cm^2. This is equivalent to a thickness

of 650 nm for dense, dry, amorphous UO_3, assuming a density of 7.29 g/cm^3 and a formula weight of 286.1 g/mol. This thickness is consistent with the estimate from the off-normal SEM images. The RBS spectrum collected after the light anneal showed that the O:U ratio was reduced to 3.8, but the UO_3 constituent had the same areal density. This implies a reduced water content, i.e., the film's composition changed to $[UO_3]_1 + [H_2O]_{0.8} + Fe_{0.2}$.

A blow-up of the oxygen region collected from the as-grown sample is shown in Fig. 9, along with two simulated spectra. These data could only be modeled properly if it was assumed that a 40 nm thick intermediate layer of Fe_2O_3 existed between the uranium oxide film and the Fe substrate (assuming a Fe_2O_3 density of 5.24 g/cm^3 and a formula weight of 159.7 g/mol). Note that the intermediate layer was unaffected by the light anneal. This Fe_2O_3 could be attributed partly to the native oxide present on the Fe foil surface before reaction, and partly to the corrosion and further oxidation of the Fe substrate while in solution. Unfortunately, we do not have a measure of the thickness of the native oxide present before reaction, so we cannot estimate the extent of the additional oxidation.

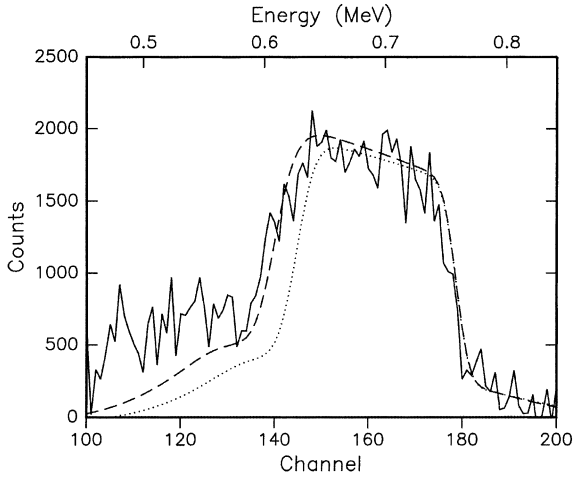

Fig. 9. Blow-up of the O peak in the RBS spectrum collected prior to annealing after subtracting off a 4th-order fit to the surrounding Fe substrate signal. Two simulations are included, one (dotted curve) reflecting only the hydrated UO_3 layer, and the other (dashed curve) also including a 40 nm thick Fe_2O_3 intermediate layer.

Additional RBS spectra were collected from another film that had been annealed in UHV at 350°C for 30 min. A spectrum collected after the 350°C anneal (solid line) is shown along with a RUMP simulation (dashed line) in Fig. 10. A blow-up of the O region is shown in Fig. 11. The shapes of both the U and O

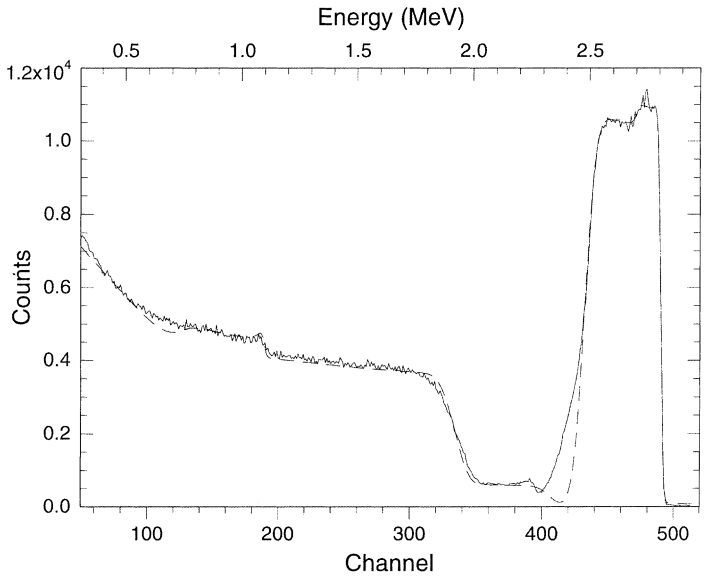

Fig. 10. RBS spectrum collected from another uranium oxide film after it was annealed in UHV at 350°C (solid line), shown along with the RUMP simulation of UO_x normalized to the Fe substrate signal (excluding the "exposed" Fe).

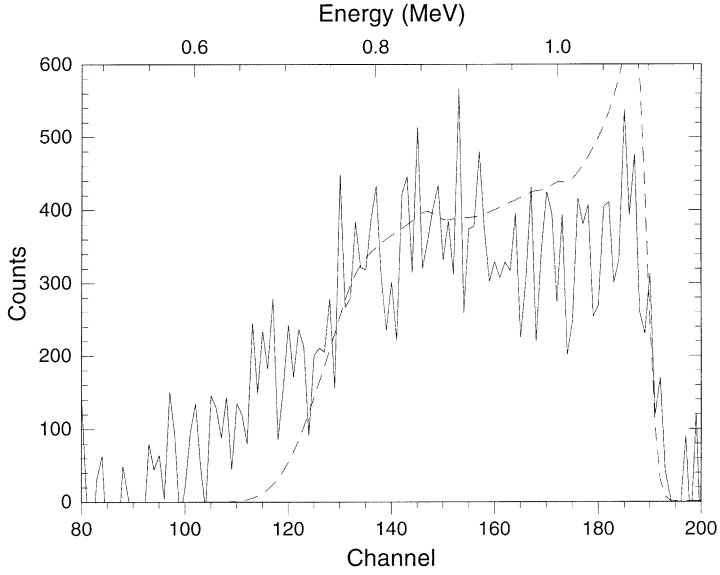

Fig. 11. Blow-up of the O peak in the RBS spectrum collected from the same sample as used for Fig. 10 along with a simulation of the data. The simulation appears to exceed the data, suggesting the presence of an additional constituent in the real film, which is most probably H.

peaks suggest that there are two regions in the film following the 350°C anneal. Because the counting statistics were inadequate to isolate the oxygen peak by subtracting the substrate signal (i.e., by fitting the substrate signal with a polynomial and interpolating), the oxygen level was roughly estimated by normalizing the spectrum to the Fe substrate signal (defined as the difference between the total Fe substrate signal and the "exposed Fe") and reducing the height of the U peak by diluting the U with O. The analysis showed that the upper region has an areal density of 1.15×10^{18} atoms/cm^2 and O:U ratio of 3.2, while the region below has an areal density of 2.30×10^{18} atoms/cm^2 and O:U ratio of 3.6. This is consistent with the notion that annealing removes oxygen from the surface region of film. In addition, there was a 0.70×10^{18} atoms/cm^2 layer of Fe_2O_3 at the interface, which is equivalent to a thickness of 71 nm. Additional spectra were collected from an annealed sample following an overnight exposure to air at room temperature. No significant changes were observed in the spectra as a consequence of the air exposure.

The bulk crystal structure of the uranium oxide film at various stages was probed by XRD. The XRD spectrum shown in the top panel of Fig. 12 was collected from a newly grown film, the middle panel was collected from a film that had been heated in vacuum, and the bottom panel was collected from the heated sample after exposure to air for 5 days. The same sample was also examined after 3 weeks of exposure to air (data not shown). The as-grown film was unidentifiable from XRD, as no peaks other than those from Fe substrate are evident in the spectrum. This indicates that the as-grown film has a very poor crystallinity, i.e., it is amorphous. When the film was heated to 450°C in vacuum for 10 min, however, several peaks appeared suggesting that the film had crystallized. It should be pointed out that these peaks do not exactly correspond to any of the common U(VI) minerals [15,16]. The closest match to the *d*-spacings are those from the mineral phase of $UO_{2.25}$ or U_4O_9 [15,16]. This mineral is primarily a U(IV) oxide and the most commonly found composition for the mineral "uraninite" [17]. Thus, it can be concluded that upon heating in vacuum, the film reduces to U(IV), consistent with the XPS and NEXAFS results, and also at least partially crystallizes. After exposure to air, the XRD spectra were unchanged, which suggests that bulk crystal structure

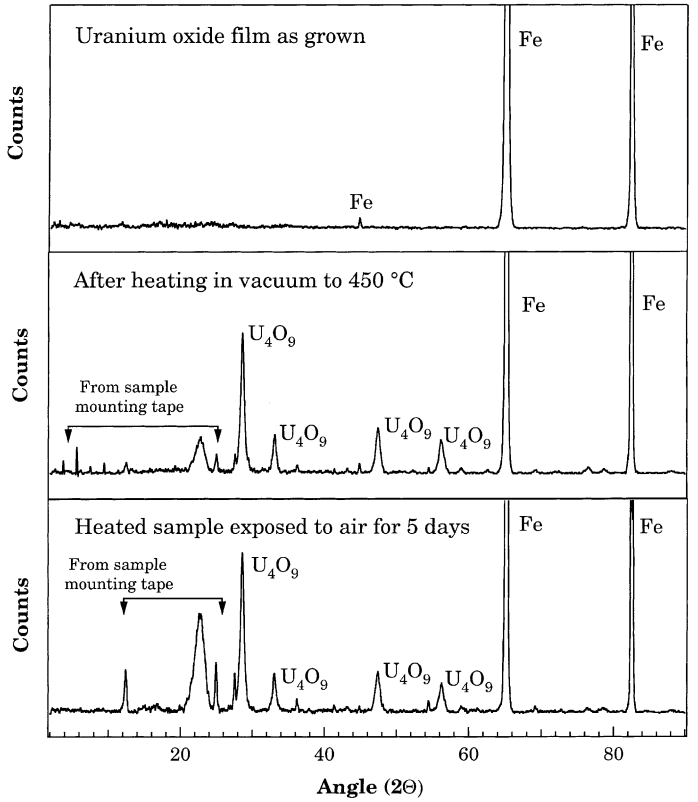

Fig. 12. XRD spectra collected from the uranium oxide films at various stages.

is unaffected, although XPS shows that the surface region re-oxidizes to U(VI).

Fig. 13 shows two LEIS spectra collected from the uranium oxide film. LEIS is sensitive to the elemental composition of the outermost atomic layer. The lower spectrum was obtained after the as-grown sample was heated to 370°C in UHV for 1 min. As expected, peaks that represent single scattering from U and O are apparent. A small Fe signal was also detected, however. The upper spectrum was obtained from a sample that was put through many cycles of water adsorption and desorption by annealing at 450°C (the water adsorption was performed for another experiment, and is not relevant here). In this case, the intensity of the Fe peak increased significantly. The increase in scattering from Fe suggests that more of the substrate became exposed when the sample was heated at the higher temperature. This is consistent with the SEM results, in which the size of the cracks on the surface increased as the sample was annealed.

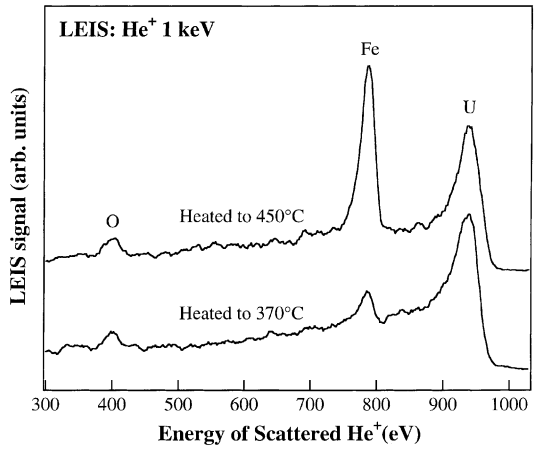

Fig. 13. LEIS spectra measured at room temperature from the uranium oxide film after various heat treatments. The bottom spectrum was obtained after the as-grown film was heated in UHV for 1 min at 370°C. The upper spectrum was collected after repeated sample annealing at 450°C and numerous water adsorption–desorption cycles.

4. Discussion

The results of the various techniques suggest that the as-grown film is an amorphous uranium(VI) oxide with an O:U stoichiometry of 4.5. If the film was composed of a single mineral, the most likely candidate that is consistent with this oxidation state and stoichiometry is ''partially dehydrated schoepite''. Schoepite is a common U(VI) mineral with a formula of $[(UO_2)_8O_2(OH)_{12}](H_2O)_{12}$ [17]. Schoepite has an O:U ratio of 5.25, which is somewhat greater than the RBS result indicates, however. It is known that schoepite transforms slowly in air at ambient temperature to ''metaschoepite'', $[(UO_2)_8O_2(OH)_{12}](H_2O)_{10}$, which has an O:U ratio of 5.0. When subjected to external stresses (heat, vacuum, or mechanical pressure) the metaschoepite will transform to ''dehydrated schoepite'' as follows [17]:

$$[(UO_2)_8O_2(OH)_{12}](H_2O)_{10} \rightarrow 8[(UO_2)O_{0.25}(OH)_{1.5}] + 10H_2O \quad (1)$$

Dehydrated schoepite has an O:U ratio of 3.75:1, which is less than the 4.5 U:O ratio found from the RBS data. Thus, it is likely that the film is a partially dehydrated schoepite, $[(UO_2)_8O_2(OH)_{12}](H_2O)_6$, with only short-range order.

The mechanism for growing such a thick amorphous film of U(VI) oxide on a Fe substrate is not completely known. It appears most likely that oversaturation at the surface of the iron with respect to a U(VI) oxyhydroxide phase caused surface precipitation. The 1.0 mM solutions (pH 5) that were used to grow the film are slightly oversaturated with respect to schoepite (saturation index = 0.26) based on the chemical speciation model MINTEQA2 [18]. The thermodynamic database for this program may be incomplete, however, and there is an additional ion pairing and polymerization that has not been taken into account. Also, the solutions did not show signs of precipitation upon aging.

If oversaturation is the sole driving force for the film growth, then any heterogeneous boundary that exists in the solution should also result in precipitation. To investigate this possibility, W and Mo foils were reacted in solutions under the same conditions that produced the thick uranium oxide films on Fe [19]. The W and Mo foils were first sputter cleaned with Ar^+ in UHV to remove most of the native oxide, and then exposed to air for 15 min prior to reaction. Thick uranium oxide films did not form on either W or Mo, however, after reaction times of up to 3 h. Thus, there must be another mechanism responsible for the thick film formation on the Fe foil surface.

There are two possible explanations for the film growth mechanism that are specific to Fe. The first is that the local pH in the vicinity of the Fe surface is higher than in the bulk of the solution, which would make uranium hydroxide precipitation possible only in the vicinity of the surface. The continuous corrosion of the Fe in solution in the absence of oxygen could contribute to the increase in the local pH according to the following reaction:

$$Fe^0 + 2H_2O \rightarrow Fe^{2+} + 2OH^- + H_2 \quad (2)$$

Thus, locally high pH at the iron surface could have resulted in the precipitation of an amorphous uranium hydroxide. The second possibility is that the reaction that initiated the uranium precipitation is the oxidation of the Fe by uranyl, according to the following equation:

$$Fe^0 + UO_2{}^{2+} \rightarrow Fe^{2+} + UO_2\,(s) \quad (3)$$

In this case, a thin film of UO_2 (s) would have formed on the surface of the iron and would have served as a template for uranyl hydroxide precipitation.

It has generally been accepted that the reaction of uranyl with ZVI is via reduction and precipitation of a U(IV) oxide [7,20]. According to the second scheme, this reaction initiates the precipitation of the thick layer of U(VI) oxide. The thin layer of UO_2 acts as a nucleation surface for the continuous precipitation of the amorphous U(VI) oxide. Evidence for this mechanism can be found in studies of uraninite oxidation. When uraninite (UO_2 (s)) oxidizes to U_4O_9, there is a slight mismatch in the unit-cell parameters between the two crystal phases [4]. However, the ''fit'' is sufficiently good that the U_4O_9 will form on UO_2, with a somewhat weakened grain boundary. It is likely that the ''amorphous'' uranyl oxide that we observe is a transition phase that more closely matches the unit-cell spacing of the UO_2 template. Electrochemical investigations of the oxidation of U_4O_9 to U_3O_7 reported the development of a 5–10 nm thick U_3O_7 surface layer [4]. It is important to note that the difference between the unit-cell parameters for U_4O_9

and U_3O_7 are small, but a large degree of cell expansion and recrystallizaton occurs upon continued oxidation to U_3O_8 [21]. The reason for not observing the layer of reduced U in the XPS spectra would be attributed to the fact that the "schoepite film" is too thick. In addition, the amount of U(IV) would be negligible compared to the amount of uranium in the bulk of the film so that the bulk-sensitive techniques employed, such as NEXAFS, are not sensitive enough to detect it.

Thermodynamic calculations show that all of the metals, Fe, W, and Mo, should be oxidized by the uranyl ion. The oxidation of Fe by uranyl has been observed, indicating that there are no activation barriers or kinetics problems to this reaction. From our limited studies, however, we have no indication that the reaction occurs with either W or Mo. This is attributed to passivate oxide layers on the metals or to kinetic inhibitions associated with high activation barriers that make the reaction exceedingly slow. The W and Mo metal surfaces did not react with the uranyl and the precipitation of the amorphous U(VI) oxide therefore did not have the proper nucleating surface or locally high pH.

It thus appears that either a locally high pH at the surface of the iron or an initial redox reaction is likely responsible for initiating the amorphous schoepite precipitation. Further investigations are underway in our laboratory to explore the possible growth mechanisms and the conditions which favor U(VI) reduction by iron metal [19].

The similarity in morphology before and after heating, as evident in the SEM images, might suggest that the heated film has a similar crystal structure as the as-grown film. The XRD spectra collected from the as-grown film, however, indicate an amorphous phase. Because the O:U ratio decreases upon heating in vacuum, it is likely that water and oxygen evaporate from the film and the atoms rearrange locally; XRD measurements show that at least a fraction of the reduced film is U_4O_9. Thus, there is no massive diffusion of U atoms throughout the film, which explains why there is little change in morphology upon heating other than the enlarged cracks. Note that the multi-layer structure showed in Fig. 10 indicates that a longer annealing time is actually needed to convert the entire film to the reduced form.

The thermally activated reduction of scheopite causes oxygen to diffuse through the film, but oxygen is not expected to react preferentially at the interface with Fe because of the thermodynamic barrier. The ΔH_f per O atom for scheopite is estimated at $-419\ \mathrm{kJ\ mol^{-1}}$ [22], while the ΔH_f for Fe_2O_3 is about $-275\ \mathrm{kJ\ mol^{-1}}$ per O atom [23]. Even the removal of one of the water groups from scheopite would consume about $300\ \mathrm{kJ\ mol^{-1}}$ [22]. Thus, it is thermodynamically uphill to move oxygen from the uranium film and react it with the underlying Fe metal. The increased thickness of the Fe_2O_3 layer after annealing that was determined from the RBS data is most likely because the two measurements were performed on different samples.

The trace amount of Fe estimated from RBS data and seen with LEIS can be explained by the cracks present in the films. The open regions expose the Fe substrate to the incoming ions. The small number of cracks in the as-grown film could result from a loss of water, since the samples were stored in a vacuum desiccator for an extended period of time after growth. This notion is supported by the fact that cracks were not seen in another sample that was stored in air, but did appear on that sample after it was heated in vacuum (data not shown), since heating does initiate the loss of water. Thus, it is possible for a sample to be placed under vacuum for only a short period of time, so that the cracks have not yet formed.

In order to use these samples as substrates for certain other experiments, it is important to grow them without cracks so that the Fe substrate is not exposed. For the U(VI) oxide, this can be accomplished by maintaining a moist environment. For the U(IV) oxide, however, this is more difficult as it is formed by heating in vacuum. A possible method for producing a uniform U(IV) oxide would be to alternate cycles of growth and annealing. First, a U(VI) film would be grown in solution. Then it would be annealed in vacuum to reduce the film to U(IV), but this would induce pinholes. The pinholes could then be filled in with an additional film growth step. This would be followed by another annealing, and so on. Such a process may enable the production of a U(IV) film without the presence of cracks. However, this has not yet been tested and it has also been shown that dehydrated schoepite may inhibit the reprecipitation

of schoepite [24]. It is also important to note that the dehydration of schoepite is irreversible [17].

5. Summary

A novel method was discovered for growing uranium oxide films onto Fe surfaces from solution. The as-grown films are a amorphous U(VI) oxide with incorporated water. After annealing in vacuum, the films reduce to U(IV). Although the surface will oxidize in air to U(VI), the bulk of the U(IV) films are inert to re-oxidation. These methods provide a unique way to make quality films of U(VI) and U(IV) in a safe, economical manner. The chemical compositions of films are very similar to those of spent nuclear fuel materials. The success of this work has great promise for enabling various fundamental and applied studies of uranium oxide surfaces.

Acknowledgements

The authors would like to thank Dr. K. Bozhilov for providing the access to the Analytical Electron Microscopy Facility in the Institute of Geophysics and Planetary Physics (IGPP) at the University of California, Riverside, and most importantly, for valuable discussions. The authors are grateful to the staff at the Stanford Synchrotron Radiation Laboratory (SSRL) for the support in performing the NEXAFS experiment. SSRL is funded by the US Department of Energy, Office of Basic Energy Sciences under Contract DE-AC03-76SF00515. The authors also acknowledge beneficial discussions with Mr. B. Corbitt while preparing the manuscript.

This work was supported by the US Department of Energy, Environmental Management Science Program (DE-FG07-96ER14707, UCR; DE-FG07-97ER14833, Rutgers). Partial support was given by the Director, Office of Science, Office of Basic Energy Sciences, Division of Materials Sciences of the US Department of Energy under Contract No. DE-AC03-76SF00098. SRQ acknowledges support from the National Science Foundation IGERT program (DGE-9554506).

References

[1] D.J. Wronkiewicz, E.C. Buck, in: P.C. Burns, R. Finch (Eds.), Uranium: Mineralogy, Geochemistry, and the Environment, Reviews in Mineralogy, Vol. 38, Mineralogical Society of America, 1999, p. 475.
[2] P. Taylor, D.D. Wood, D.G. Owen, J. Nucl. Mater. 223 (1995) 316.
[3] P. Taylor, R.J. Lemire, D.D. Wood, Nucl. Technol. 104 (1993) 164.
[4] L.H. Johnson, D.W. Shoesmith, in: W. Lutze, R.C. Ewing (Eds.), Radioactive Waste Forms for the Future, Elsevier, Amsterdam, 1988, p. 635.
[5] E.K. Wilson, Chem. Eng. News 73 (1995) 19.
[6] S.R. Qiu, H.-F. Lai, M.J. Roberson, M.L. Hunt, C. Amrhein, L.C. Giancarlo, G.W. Flynn, J.A. Yarmoff, Langmuir 16 (2000) 2230.
[7] J.N. Fiedor, W.D. Bostick, R.J. Jarabek, J. Farrell, Environ. Sci. Technol. 32 (1998) 1466.
[8] M.C. Duff, C. Amrhein, Soil Sci. Soc. Am. J. 60 (1996) 1393.
[9] M.N. Hedhili, B.V. Yakshinskiy, T.E. Madey, Surf. Sci. 445 (2000) 512.
[10] J.I. Goldstein, Scanning Electron Microscopy and X-ray Microanalysis: a Text for Biologists, Materials Scientists, and Geologists, Plenum Press, New York, 1992.
[11] P.M. Bertsch, D.B. Hunter, S.R. Sutton, S. Bajt, M.L. Rivers, Environ. Sci. Technol. 28 (1994) 980.
[12] F. Farges, C.W. Ponader, G. Calas, G.E. Brown Jr., Geochim. Cosmochim. Acta 56 (1992) 4205.
[13] L.R. Doolittle, Nucl. Inst. Meth. B 9 (1985) 334.
[14] L.R. Doolittle, Nucl. Inst. Meth. B 15 (1986) 227.
[15] W.F. McClune, Mineral Powder Diffraction File, Group Data Book, International Centre for Diffraction Data, Swarthmore, PA, 1993.
[16] L.G. Berry, Joint Committee on Powder Diffraction Standards in Cooperation with American Society for Testing and Materials, Vols. 6–10, Philadelphia, PA, 1967.
[17] R. Finch, T. Murakami, in: P.C. Burns, R. Finch (Eds.), Uranium: Mineralogy, Geochemistry, and the Environment, Vol. 38, Mineralogical Society of America, 1999, p. 91.
[18] US EPA, Metal Speciation Equilibrium Model for Surface and Groundwater (MINTEQA2), Version 3.11, CEAM, 1991.
[19] S.R. Qiu, C. Amrhein, J.A. Yarmoff, Unpublished.
[20] J. Farrell, W.D. Bostick, R.J. Jarabek, J.N. Fiedor, Ground Water 37 (1999) 618.
[21] R.J. Finch, R.C. Ewing, J. Nucl. Mater. 190 (1992) 625.
[22] T.L. Woods, R.M. Garrels, Thermodynamic Values at Low Temperature for Natural Inorganic Materials: an Uncritical Summary, Oxford University Press, New York, 1987.
[23] I. Barin, Thermochemical Data of Pure Substances, VCH, New York, 1995.
[24] R.J. Finch, M.L. Miller, R.C. Ewing, Radiochim. Acta 58–59 (1992) 433.